6-2015

Hydraulic Modeling of Glacial Dam-Break Floods on the West Branch of the Susquehanna River, Pennsylvania

Jessica Newlin
Bucknell University, jtn003@bucknell.edu

Benjamin R. Hayes
Bucknell University, brh010@bucknell.edu

AGU PUBLICATIONS

Earth and Space Science

RESEARCH ARTICLE
10.1002/2015EA000096

Key Points:
- Potential paleofloods are simulated on the West Branch Susquehanna River
- Hydraulic model results support Pleistocene glacial dam-break hypotheses
- Important hydraulic differences are found between modern floods and paleofloods

Correspondence to:
J. T. Newlin,
jessica.newlin@bucknell.edu

Citation:
Newlin, J. T., and B. R. Hayes (2015), Hydraulic modeling of glacial dam-break floods on the West Branch of the Susquehanna River, Pennsylvania, *Earth and Space Science*, *2*, 229–243, doi:10.1002/2015EA000096.

Received 9 JAN 2015
Accepted 2 JUN 2015
Accepted article online 8 JUN 2015
Published online 7 JUL 2015

Hydraulic modeling of glacial dam-break floods on the West Branch of the Susquehanna River, Pennsylvania

Jessica T. Newlin[1] and Benjamin R. Hayes[2]

[1]Civil and Environmental Engineering, Bucknell University, Lewisburg, Pennsylvania, USA, [2]Watershed Sciences and Engineering Program, Bucknell University Center for Sustainability and the Environment, Lewisburg, Pennsylvania, USA

Abstract This study investigates the potential hydraulic conditions of catastrophic floods in the West Branch of the Susquehanna River (West Branch) during the middle to late Pleistocene period and the influence of these paleofloods on the current river bed form. The current channel bed form is characterized using sonar bathymetry data collection techniques. The paleofloods are hypothesized based on published geological evidence of early Pleistocene glacial Lake Lesley in the West Branch Valley, which was formed by a glacial ice dam that potentially failed during mild climate cycles in the Pleistocene period. A one-dimensional, steady hydraulic model is developed to simulate estimates of paleoflood peak discharges and the modern 100 year return period peak discharge. The computed water-surface profiles, shear stresses, and flood inundation maps could explain the erosional and depositional features identified by other researchers as being formed during the Pleistocene and could explain features revealed by the bathymetry data. Therefore, the hydraulic modeling results support previously inferred hypotheses of the occurrence of glacial dam-break floods on the West Branch of the Susquehanna River. The differences that are evident between the paleoflood simulations and the simulation of the modern 100 year peak discharge are attributable to valley constrictions that cause substantial backwater effects for the larger paleoflood discharges but not for the lower modern flood discharge volume. The ability to simulate potential paleofloods in the West Branch of the Susquehanna River complements the paleostage indicator work done by other researchers and enables innovative analysis of glaciofluvial processes and their effect on the current river bed form.

1. Introduction

Paleofloods are often investigated in the context of catastrophic floods or megafloods [*Baker*, 2009]. These high-magnitude floods leave behind geological evidence or paleostage indicators of the water levels and flow hydraulics that are not easily "erased" by modern-day natural or anthropogenic activities. Several paleofloods have been studied worldwide [e.g., *Rudoy*, 2002; *Alho et al.*, 2005; *Sheffer et al.*, 2008; *Kochel et al.*, 2009; *Alho et al.*, 2010; *Carling et al.*, 2010; *Denlinger and O'Connell*, 2010; *Meinsen et al.*, 2011; *Kasse*, 2014]. These studies involved the identification of paleoflood indicators [*Rudoy*, 2002; *Sheffer et al.*, 2008; *Kochel et al.*, 2009; *Meinsen et al.*, 2011; *Kasse*, 2014] and modeling of estimated paleoflood discharges [*Alho et al.*, 2005, 2010; *Carling et al.*, 2010; *Denlinger and O'Connell*, 2010] to characterize the effects of the mega-floods on the observed landscapes.

Current glaciation can lead to the creation of megafloods (jökulhlaups) in some regions of the world, which enable investigation of water flow through glaciers and provide supplementary information for simulating paleofloods. For example, the mechanisms of the generation of modern glacial outburst floods and the estimation of the flood magnitude have been covered by *Driedger and Fountain* [1989], *Mayo* [1989], *Motyka and Truffer* [2007], and *Hewitt and Liu* [2010]. *Fountain and Walder* [1998] summarize the general flow of water through temperate glaciers, including a description of potential glacial outburst flood initiation mechanisms. *Roberts* [2005] focuses on Icelandic jökulhlaups to more specifically assess floodwater flow through glaciers and summarize the development of mathematical and empirical models to simulate the flood processes. More recently, *Carravick and Tweed* [2013] provide an analysis of proglacial lakes including the geological evidence of glacial lake outburst floods. Modern glacial outburst flood events also have provided hydraulic and geomorphic modeling opportunities. For example, *Klimeš et al.* [2014] and *Cenderelli and Wohl* [2001] use one-dimensional hydraulic modeling and observed flood stage indicators to estimate the hydraulic processes and peak discharges of glacial outburst floods formed by moraine dam failures in Peru and in the Mount Everest region, respectively. The geomorphic effects of the modeled floods in the Mount Everest region are summarized by *Cenderelli and Wohl* [2003]. *Bohorquez and Darby* [2008] assess the use of one-dimensional and two-dimensional hydraulic modeling to reconstruct a 1943 outburst flood in Switzerland.

Similar to the modeling of modern glacial outburst floods, several studies have applied a range of flow models to simulate paleofloods based on paleostage indicators. Flood stage indicators were used as a means to calibrate a Holocene glacial outburst flood in northeast Iceland using a one-dimensional hydraulic model [*Alho et al.*, 2005]. *Alho et al.* [2010] reconstructed the largest glacial Lake Missoula draining using three drainage scenarios and an unsteady two-dimensional hydraulic model. *Denlinger and O'Connell* [2010] also simulated outburst floods from glacial Lake Missoula with a two-dimensional shallow-water flow model and dam-break scenarios. Where adequate geomorphological and sedimentological data are available to calibrate a two-dimensional model, *Carling et al.* [2010] found that both one-dimensional and two-dimensional unsteady flow simulations can provide valuable insight into paleoflood dynamics. With respect to areal flood inundation simulation, *Alho and Aaltonen* [2008] show that one-dimensional and two-dimensional hydrodynamic models result in similar predictions especially along simple flow paths in the flatter, central area of a floodplain.

2. Glaciation and the West Branch of the Susquehanna River

The West Branch of the Susquehanna River (West Branch) watershed drains a 17,734 km^2 area in the Valley and Ridge Province and Allegheny Plateau Province of north-central Pennsylvania. The landscape morphology of this region generally reflects the erosional forces and progressive lowering by glaciation and fluvial processes balanced by the resistance of bedrock lithology and geologic structures over millennia. More recently, during the Pleistocene period, Laurentide continental ice sheets extended into the upper reaches of the West Branch once during the Illinoian glacial stage and at three different times during the Wisconsinan glacial stage [*Peltier*, 1949; *Sevon et al.*, 1999].

Resistant sandstone units of the Bald Eagle anticline likely control the regional slope of the river and direct its flow west to east from Lock Haven, PA, to Williamsport, PA, to Muncy, PA (Figure 1). At Muncy, the river abruptly curves south as the resistant bedrock fold plunges beneath the river. For the next 45 km, until its confluence with the North Branch at Northumberland, PA, the West Branch flows perpendicular to geologic structures, exposing bedrock cliffs near Montgomery, Watsontown, and Milton. The major transverse drainages (gorges cut through resistant rock ridges by streams) on the Susquehanna River have been associated with the Paleozoic age, 400 Ma [*Lee*, 2013].

The West Branch flows through a 0.5 to 2 km wide bedrock valley overlain by up to 10 to 25 m of predominantly glaciofluvial outwash alluvium [*Nelson*, 1965; *Engel et al.*, 1996] with several alluvial terraces discernable on the valley floor [*Peltier*, 1949; *Nelson*, 1965; *Marchand and Crowl*, 1991; *Engel et al.*, 1996; *Kochel et al.*, 2009]. These studies have determined this alluvium to be glaciofluvial in origin, with imbricated boulders that exceed the size of material that could be transported by modern floods. Additional geological evidence shows the deposits to be younger than two million years, presumably deposits by meltwaters from continental ice sheets that prograded into the West Branch Valley during the Pleistocene. *Kochel et al.* [2009] showed that in some cases, lobes of ice-dammed tributaries on the west side of the West Branch and formed glacial lakes in tributary valleys with a total storage volume of approximately 2.3 km^3. Middle Pleistocene paleofloods from these smaller tributary lakes formed steep jökulhlaup surfaces in these tributary valleys [*Kochel et al.*, 2009]. The largest Pleistocene glacial lake known to have existed in this region (glacial Lake Lesley) was formed when ice sheets dammed the West Branch of the Susquehanna River during the early Pleistocene (770 to 970 ka). *Ramage et al.* [1998] mapped the extent of glacial lacustrine deposits to show that glacial Lake Lesley extended over 100 km in length and 100 m in depth with an estimated maximum storage volume of 100 km^3. As demonstrated by other studies [e.g., *Kochel et al.*, 2009; *Alho et al.*, 2010; *Carling et al.*, 2010; *Denlinger and O'Connell*, 2010], the catastrophic failure of glacial ice dams can influence the geomorphology of the valley when large amounts of water, ice, and sediment are transported downstream.

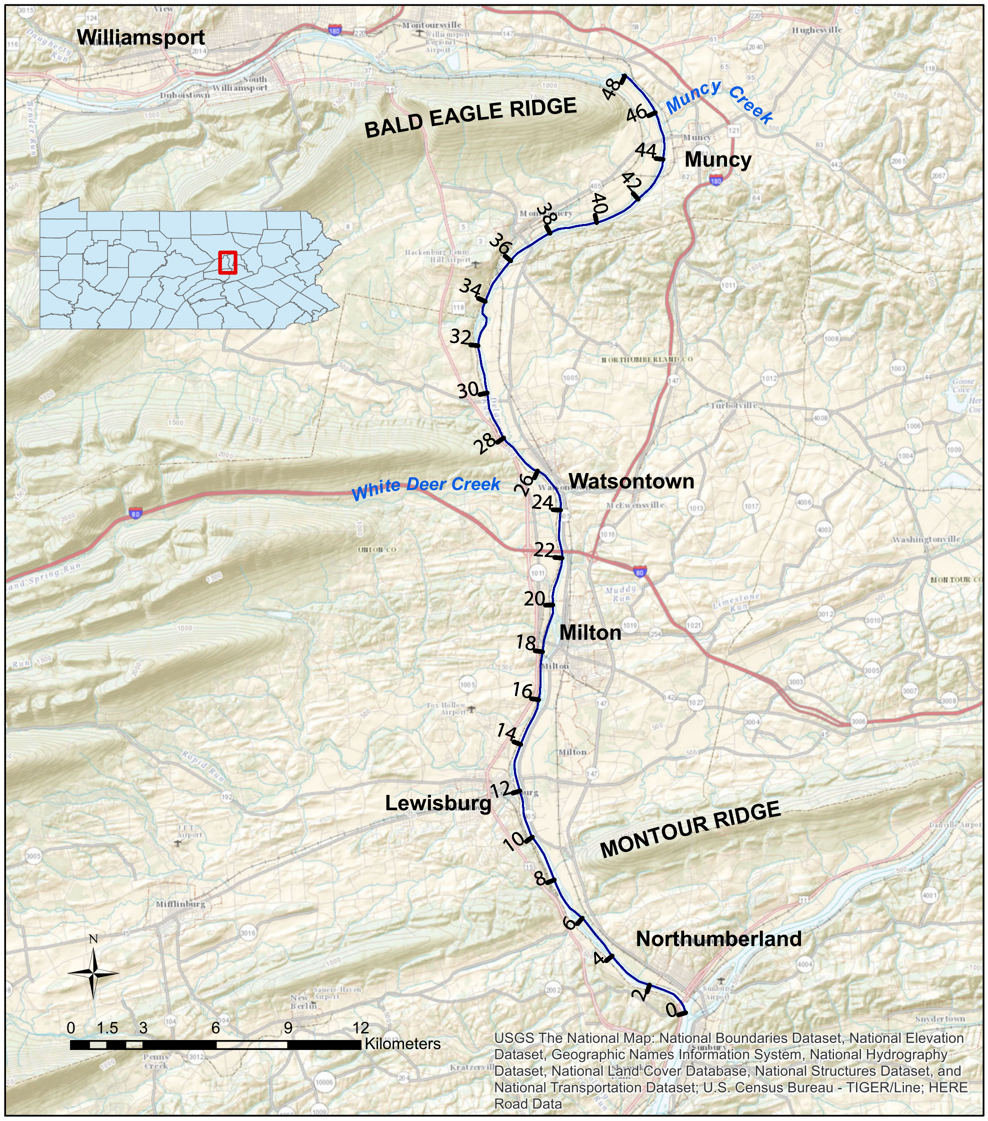

Figure 1. Location map of study reach on the West Branch of the Susquehanna River. River kilometers are labeled and measured from the confluence with the North Branch of the Susquehanna River at Northumberland, PA, along the modern channel centerline.

3. Objective

The goals of this study are to investigate the potential hydraulic conditions of catastrophic floods in the West Branch of the Susquehanna River during the middle to late Pleistocene period and to identify the influence of paleofloods on the current river bed form. Much of the previous work on characterizing the glaciofluvial processes of West Branch of the Susquehanna River [*Peltier*, 1949; *Nelson*, 1965; *Marchand and Crowl*, 1991; *Engel et al.*, 1996; *Ramage et al.*, 1998; *Kochel et al.*, 2009] has focused on the geological evidence and larger-scale paleostage indicators preserved on the floodplain and in the tributary watersheds with some investigation of bed sediments. Therefore, it was necessary to map the current channel river bed using bathymetry data collection techniques to identify river bed form features. The study focuses on a 46 km reach of the West Branch between Muncy, PA, and Northumberland, PA (Figure 1). Potential paleoflood peak discharges are determined based on empirical relationships developed by *Walder and Costa* [1996] and estimated dimensions of glacial Lake Lesley reported by *Ramage et al.* [1998]. The current terrain is constructed from the channel morphologic data combined with the valley morphologic data (lidar

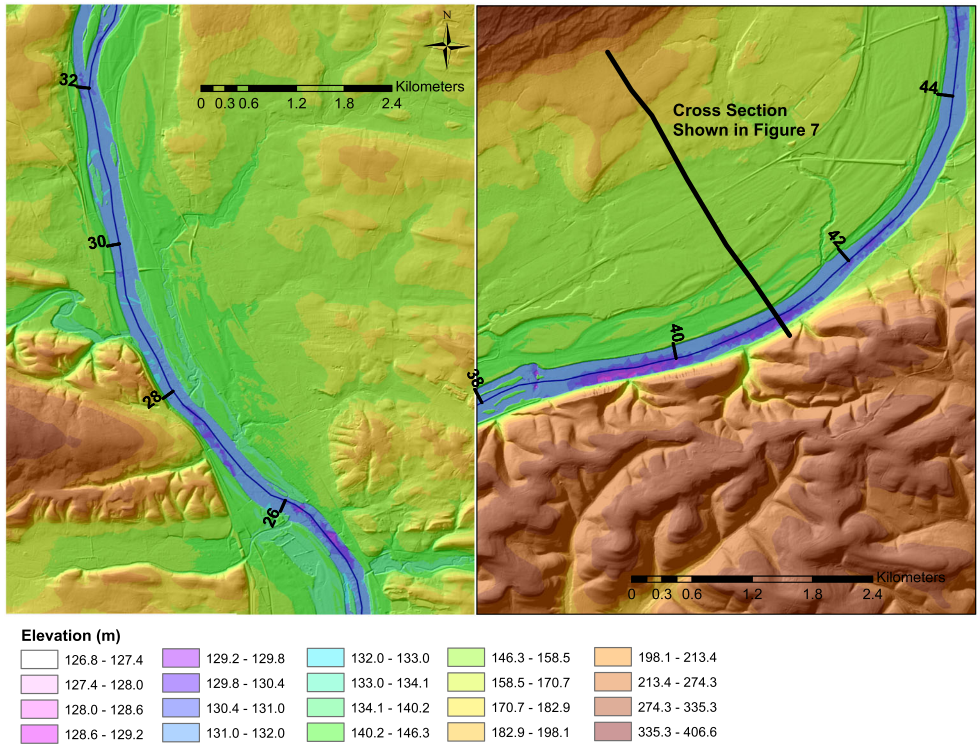

Figure 2. Multiscale geomorphic features revealed by geoprocessing of bathymetry and lidar data. Elevations 132 m and below on the graphic (blue and purple areas) are based on the geoprocessed bathymetry data and the remaining areas are based on lidar data. River kilometers (RK) are included for location reference.

coverages). The estimated peak paleoflood and modern discharges are applied to the current terrain of the West Branch with the one-dimensional, steady flow Hydrologic Engineering Center-River Analysis System (HEC-RAS) hydraulic model [*Brunner*, 2010]. The modeling results are compared with geological evidence in the form of paleostage indication data from various sources [*Peltier*, 1949; *Engel et al.*, 1996; *Marchand and Crowl*, 1991] and the collected channel bed feature data. In addition, the model results with the peak glacial dam-break discharge estimates are compared with the model results with the modern 100 year peak flood to identify bed form and river characteristics that could be a result of catastrophic paleofloods rather than modern floods.

4. Characterization of Multiscale Geomorphic Features

Channel morphology and river bed forms in the West Branch of the Susquehanna River were mapped using a high-resolution 455 kHz Lowrance 83 kHz HDS-10 Gen2 depth finder as well as a differential GPS unit to collect over 100,000 precise depth and location readings [*Newlin et al.*, 2013]. From above Muncy, PA, to the Adam T. Bower inflatable dam in Sunbury, PA, the river was longitudinally traversed in a zigzag pattern with an average cross-sectional spacing of 30 to 60 m. The sonar depths were converted to river bed elevations using time-synchronous stage data recorded at five U.S. Geological Survey gage stations along the study reach. Bank heights, water-surface variations, and channel bed features were carefully noted by the boat operator, both on the map and on GPS-tagged photographs. The data were then processed with ArcGIS to produce digital bathymetry maps by interpolating converted elevations into a gridded 5 m raster and combining this raster with terrestrial lidar data of the adjacent floodplain areas and of several midchannel islands. Pools, riffles, and channel bars visible in the bathymetry maps were confirmed by the field notes and photographs. Figure 2 shows several of the features that were revealed as a result of the geoprocessing of bathymetry and lidar data. The pink and darker purple colors in the channel represent deeper pools that were revealed by the collected bathymetry data. Channel evolution also is demonstrated in Figure 2 (right) on the right floodplain (looking downstream) as revealed by the lidar data.

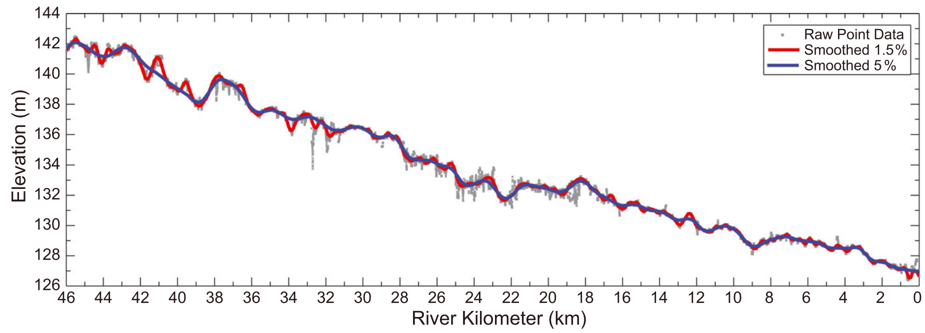

Figure 3. Longitudinal profile plot of the channel bed of the West Branch of the Susquehanna River from Muncy, PA to Northumberland, PA. River kilometers on the *x* axis refer to those labeled along the modern channel centerline in Figure 1.

The collected bathymetry data allow further investigation of the longitudinal bed profile of the current West Branch of the Susquehanna River. The detailed bed profile reveals several scales of variability in the channel bed features (Figure 3). This profile is created along the modern thalweg of the West Branch channel and the distance corresponds to the river kilometers (RK) labeled in Figure 1. The raw sonar data have considerable variability in the reaches RK 46–43, RK 38–36, RK 33–31, and RK 28–18. The sonar technology can resolve features as small as cobbles; therefore, to indicate river bed form features, smoothing of the raw sonar data is required. To delineate larger bedforms on the scale of 2 to 10 m, the data were smoothed using a robust local weighted least squares regression and a second-degree polynomial model. Two degrees of smoothing are applied: smoothing considering 1.5% of the data and smoothing considering 5% of the data. The variability in pool and riffle spacing with the two degrees of smoothing suggests that there may be multiple scales of bed features formed by multiple scales of flow regimes. Some reaches have large bed features for both degrees of smoothing (such as RK 23 in Figure 3). Exceptions to the fairly regular pool spacing for both degrees of smoothing are observed downstream of Muncy (RK 43–39) and upstream of Milton (RK 25–RK 19). The bed profile created by smoothing 5% of the data also shows very little pool-riffle variation downstream of Milton (RK 18) and between RK 25 and 28.

5. Geological Evidence of Paleofloods and the Modern Flow Regime

The geological evidence of the erosional and depositional features created by paleofloods on the West Branch are documented by *Peltier* [1949], *Nelson* [1965], *Faill* [1979], *Marchand and Crowl* [1991], *Engel et al.* [1996], *Inners* [1997], *Ramage et al.* [1998], *Hayes* [2001], and *Kochel et al.* [2009]. The observed channel bed and floodplain features are useful for comparing modern flood and paleoflood influences.

The present-day bankfull estimate of the West Branch of the Susquehanna River channel averages 270 m wide and 4 m deep, with 1–3 m high vertical banks, underlain by sand and silt overbank deposits and covered by vegetation. Braided river features, such as large bars (now islands in the main channel) and abandoned paleochannels are clearly visible on the lidar images of the valley floodplain. For example, Figure 2 (right) reveals evidence of channel evolution downstream of the proposed glacial dam-break location. The modern flow regime is incapable of forming these paleochannels, many of which are located 120 to 400 m laterally and 5–8 m vertically higher than the modern channel. Over time, these paleochannels were filled by overbank deposition and vegetation and now form elongate palustrine wetlands. One of these wetlands, Montandon Marsh, is located on the east of side of the Susquehanna River near Lewisburg, PA. Test borings and monitoring wells installed in this wetland found the paleochannels to be 46 m wide by 4 m deep and filled with organic-rich, silt, and fine sand [*Hayes*, 2001].

Large amounts of sand and silt generally are absent from the modern river bed. Preliminary pebble count data from several locations near Milton, PA, indicate that the bed is very coarse with particle sizes ranging from small cobbles to small boulders and with a median grain size between 32 and 64 mm. Extensive field observations of the channel bed have revealed that portions of the bed are bedrock and the sediment sizes on the remaining portions of the bed vary spatially; however, only limited pebble count data currently are available to indicate specific size ranges. Based on pebble count data from 18 sites on the

West Branch of the Susquehanna River, *Nelson* [1965] concluded that variability in bed sediment sizes cannot be explained completely by discharge, slope, and lithology variables. The sediment appears to be mainly well-rounded glaciofluvial outwash sediments, and based on composition and degree of weathering, they are of middle to late Pleistocene age [*Peltier*, 1949; *Nelson*, 1965].

Peltier [1949] identifies terraces along the West Branch of the Susquehanna River and correlates them to the glacial climatic regimes of the middle to late Pleistocene period with distinct cold periods (ice advances) separated by periods of mild climate, meltwater, and erosion. Along the West Branch from Lock Haven, PA, to Northumberland, PA, a series of terraces are classified [*Peltier*, 1949]: Mankato terraces (3 m height), Valley Heads terraces (5.5 m height), Binghamton terraces (8.5 m), Olean terraces (13.7 m), and Illinoian terraces (20 m). Soil chronosequences on terraces of the West Branch [*Engel et al.*, 1996] support the terrace identification of *Peltier* [1949]. Specifically, soil chronosequences developed at a site near Muncy, PA, result in a flight of seven terraces ranging in elevation from 3 m to 51 m above the modern river and ranging in age from 10 ka to 770 ka [*Engel et al.*, 1996]. Both studies [*Peltier*, 1949; *Engel et al.*, 1996] found that terrace height tends to decrease in the downstream direction suggesting that their formation through aggradation and incision could be due to catastrophic outwash events closer to the glacial advance location rather than due to large modern floods that increase in discharge in the downstream direction as contributing watershed area increases [*Peltier*, 1949].

A surficial geology map of Union and Snyder Counties in Pennsylvania [*Marchand and Crowl*, 1991] provides detailed geological evidence of the potential influences of glaciation in the valley of the West Branch of the Susquehanna River. The spatial extents of middle to late Pleistocene-aged sediment deposits are identified on this surficial geology map. Additional surficial geology maps that cover the study location provide a more general description of the spatial distribution of Pleistocene to modern-aged sediment deposits [*Faill*, 1979; *Inners*, 1997]. The spatial extent of deposits can be correlated to estimated flood inundation areas under various hydraulic conditions.

As mentioned previously, the existence of glacial Lake Lesley near Williamsport, PA, has been presented by *Ramage et al.* [1998]. The estimated age of the lake is between 770 and 970 ka, indicating that early Pleistocene glaciation blocked the West Branch of the Susquehanna River near Bald Eagle Mountain (right side of the West Branch near RK 46 in Figure 1), creating a proglacial lake that may have existed for as long as 4000 years [*Ramage et al.*, 1998]. The lake extended for over 100 km from Jersey Shore, PA, downstream past Williamsport, PA, and was as deep as 150 m and believed to have held as much as 100 km^3 of water (see Figure 4). The precise location of the ice dam is not known, but based on lake sediments, outwash gravels, and bedrock/alluvium thickness maps, the dam was likely near Bald Eagle Ridge where the West Branch begins to flow north to south near the confluence with Muncy Creek [*Sevon*, 1993; *Ramage et al.*, 1998]. It is also likely that as the climate warmed, glacial outburst floods (or jökulhlaups) from Lake Lesley occurred in the West Branch and its tributaries. As the glacial dams melted and began to fail, catastrophic releases of enormous quantities of sediment-laden water could have been transported down the river valley.

6. Glacial Dam-Break Hypotheses on the West Branch

Unraveling the history of the formation of the fluvial and topographical features of the West Branch of the Susquehanna River is a challenge because of the combination of morphologic influences ranging from prior to the Pleistocene period to modern day. In an effort to understand the hydraulic differences between the potential Pleistocene paleoflood conditions and modern flood conditions, estimates of potential discharges from the Pleistocene epoch must be identified. Conditions similar to those that may have caused paleofloods on the West Branch currently exist or have existed in recent history in some regions of the world. This enables a means to hypothesize the undocumented historical events on the West Branch. Glacial ice dams can create several types of lakes; *Costa and Schuster* [1988] cite that lakes formed in a main river valley by a tributary glacial advance are the most dangerous type. *Walder and Costa* [1996] describe ice-dam failure types as nontunnel failure and tunnel failure, with most nontunnel failures involving a breach either within the ice dam or between the ice dam and an adjacent rock wall. Given the approximate location of the ice dam that formed glacial Lake Lesley, it is feasible that the ice dam was formed by an advancing glacier from the Muncy Creek tributary into the main valley of the West Branch of

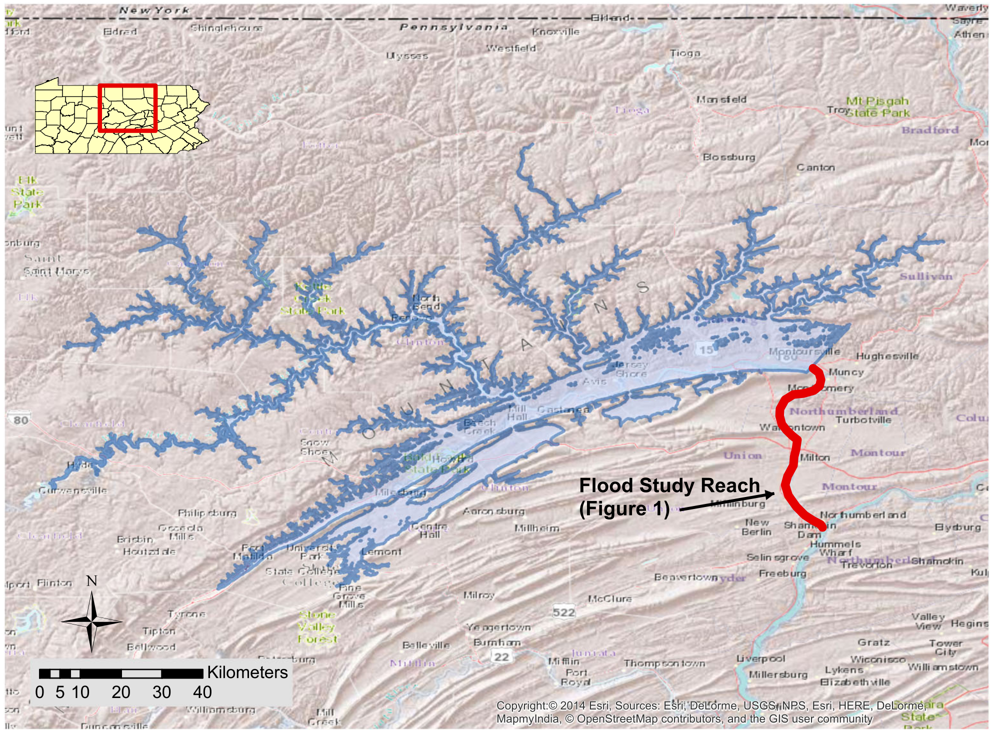

Figure 4. Estimated extents of early Pleistocene glacial Lake Lesley based on *Sevon* [1993] and *Ramage et al.* [1998]. The flood study reach is highlighted to show the difference in scale between the extent of glacial Lake Lesley and the channel that conveyed the drainage from this lake.

the Susquehanna River and butting up against Bald Eagle Mountain on the west side of the river (near RK 46 and see Figure 5). Empirical relations for estimating a peak discharge from glacier-dammed lakes [*Walder and Costa*, 1996] were applied to the estimated dimensions of glacial Lake Lesley [*Ramage et al.*, 1998] to determine plausible peak discharge values to use in a hydraulic simulation of paleofloods. Given the potential location of the ice-dam and the glacial fluctuations, it is likely that a jökulhlaup cycle [*Tweed and Russell*, 1999] was present in the West Branch.

7. Hydraulic Model Development

The HEC-geoRAS model [*Ackerman*, 2009] was used to aid in the development of a geometry model for hydraulic simulation of a range of discharges in the West Branch of the Susquehanna River. With HEC-geoRAS, 61 cross sections were developed with an average channel spacing of 800 m (Figure 5). The elevation data for the cross sections were based on a triangulated irregular network surface created from the combination of the collected bathymetry data for the channel and the lidar data for the larger valley morphology. Model simulations include modern flood as well as much larger paleoflood peak discharge estimates. Therefore, the channel cross sections were extensively defined across the valley. The cross-section geometry information was imported to the HEC-RAS model for hydraulic simulation.

The HEC-RAS model provides a one-dimensional energy and momentum solution for the water-surface profile in the West Branch channel given geometry and estimated paleoflood discharges. Two-dimensional effects, such as expansion and contraction of flow or meanders are difficult to calibrate in a one-dimensional model without experimental evidence [*Carling et al.*, 2010]; however, one-dimensional models such as HEC-RAS are successfully used to simulate two-dimensional effects of bridge hydraulic transitions with increased values for expansion and contraction coefficients and ineffective flow delineation [*Hunt et al.*, 1999]. An iterative approach was used with the West Branch HEC-RAS model to determine ineffective flow locations and cross sections where expansion and contraction losses should be increased. While detailed modern-day geometry data exist, a two-dimensional model for paleoflood discharges was

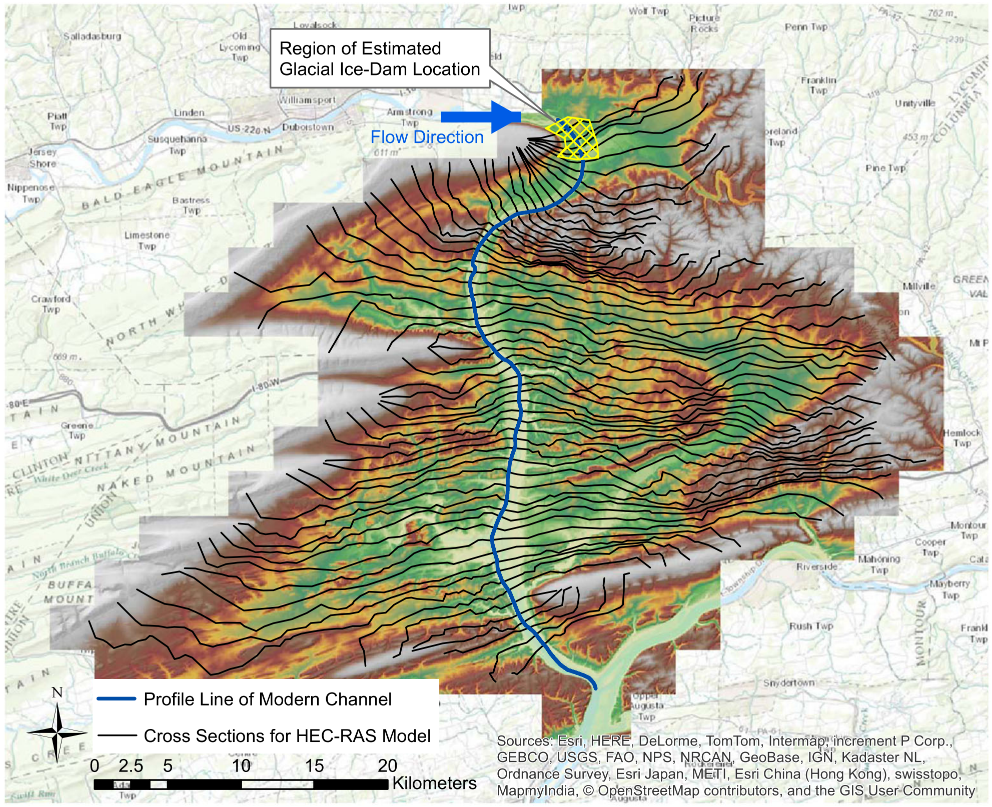

Figure 5. Cross-section delineation for HEC-RAS geometry and approximate location of the glacial ice-dam forming glacial Lake Lesley.

deemed inappropriate given the lack of known flow magnitude at this stage of the analysis of paleoflood hydraulics in the West Branch of the Susquehanna River.

Several discharge estimates for the paleoflood magnitudes (see Table 1) were simulated with the West Branch HEC-RAS geometry model. The peak flood discharges were estimated using empirical glacial ice-dam failure equations relating lake volume and discharge [*Walder and Costa*, 1996]. The maximum discharge (Breach 100% = 173,000 m^3/s) assumes that the entire volume of glacial Lake Lesley drained in a breach-type failure of the ice-dam. If the entire volume of the lake drained by tunnel failure, the peak discharge would be lower (92,000 m^3/s). Glacial dams often fail periodically, and during failure, deformation and movement of the ice can reestablish the ice-dam blockage [*Costa and Schuster*, 1988]. Therefore, the paleoflood peak discharge estimates (Table 1) are listed in terms of the percentage of the volume of the lake that would have drained given a breach-type failure. This assumes that an individual glacial dam-break event may not have drained the entire lake. Modern flood discharges were estimated based on flood frequency analyses with a log Pearson Type III distribution assumption for data from the Williamsport and the Lewisburg U.S. Geological Survey gaging stations. These analyses consider postregulation flows on the West Branch as this best represents the current flow regime.

Table 1. Peak Discharge Estimates of Modern Floods and Paleofloods on the West Branch of the Susquehanna River

Description	Discharge (m^3/s)	Discharge (cfs)	Comments
100 years	8,500	300,000	Modern 100 year return period peak discharge; approximately equal to the modern flood of record
Breach 100%	173,000	6,100,000	Estimate assuming 100% of lake volume drained during a breach failure event
Breach 25%	92,000	3,250,000	Estimate assuming 25% of lake volume drained during a breach failure event (or 100% of volume drained during a tunnel failure event)
Breach 15%	74,000	2,600,000	Estimate assuming 15% of the lake volume drained during a breach failure event
Breach 8%	57,000	2,000,000	Estimate assuming 8% of the lake volume drained during a breach failure event

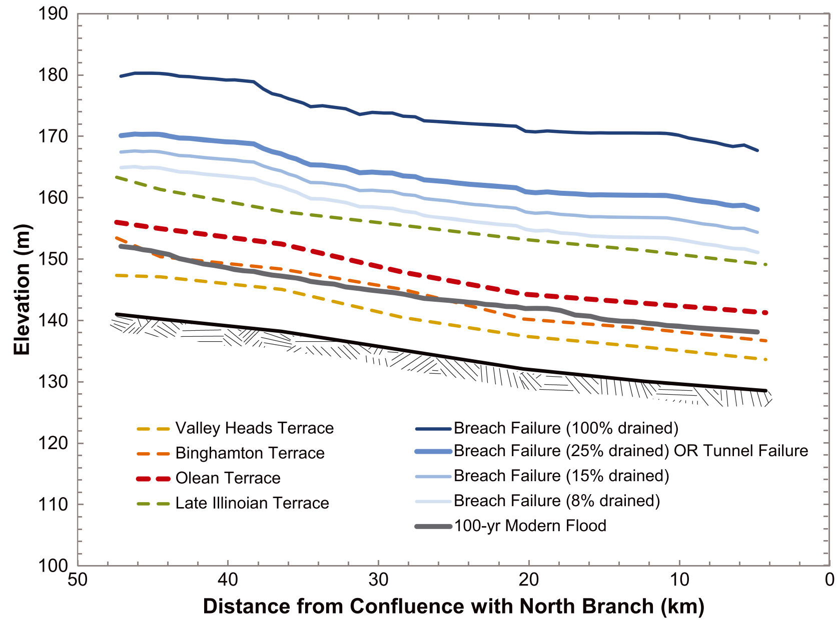

Figure 6. Computed longitudinal water-surface profiles (solid lines) plotted with middle to late Pleistocene terrace profiles (dashed lines) mapped by *Peltier* [1949].

The one-dimensional hydraulic model with the modern flood discharge was calibrated according to high water elevations recorded from the Tropical Storm Agnes flood that occurred in the Susquehanna Valley in 1972. On the West Branch of the Susquehanna River, this flood remains the flood of record and the peak discharge was approximately equal to the 100 year return period peak discharge according to flood frequency analyses with Williamsport and Lewisburg flow gage data. Therefore, the Manning's roughness values in the main channel and overbank areas could be calibrated for the modern peak flood discharge. For the paleoflood discharge estimates, the roughness value (n) could not be calibrated and a constant value was specified for the channel and floodplain, $n = 0.045$. It is assumed that the characteristics of the paleofloods were different from modern floods as they likely carried a higher sediment and ice concentration with large volumes of discharge that were not maintained within the modern channel banks or floodplain region. The chosen Manning's roughness value is similar to others used in paleoflood modeling as summarized by *Kidson et al.* [2006]. The sensitivity of the West Branch paleoflood simulations to the chosen roughness value was investigated by varying the roughness value ±10%, and the resulting differences were minor for the purposes of this analysis.

8. Results and Discussion

The HEC-RAS simulation results were compared with the geological evidence of middle to late Pleistocene paleostage indicators previously described [*Peltier*, 1949; *Marchand and Crowl*, 1991; *Engel et al.*, 1996]. This comparison required postprocessing of the results with the use of HEC-geoRAS. The following examines the resulting water-surface elevations, the channel shear stresses, and the flood inundation areas for the simulated peak discharge estimates.

8.1. Water-Surface Profiles

The calculated water-surface profiles are presented in Figure 6 and compared with terrace profiles along the West Branch developed by *Peltier* [1949]. The range of paleoflood discharges produce water-surface profiles that are above all of the estimated terrace elevations of middle to late Pleistocene age. These paleoflood profiles show a steeper water-surface profile between river kilometers 40 and 35 and a flat water-surface profile between river kilometers 18 and 10. The water-surface elevations for the modern 100 year flood discharge are lower than some of the Pleistocene terraces, and the profile does not show the same trends in steepness as the paleoflood peak discharge profiles. The water-surface profile results are presented in

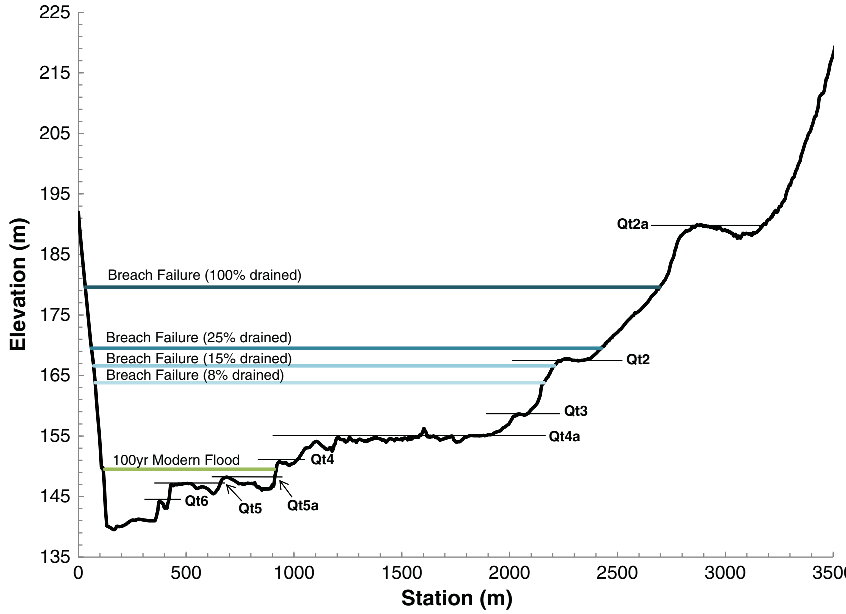

Figure 7. Cross-section view (looking downstream) showing water-surface elevations for paleoflood and modern flood discharges at river kilometer 41. Middle to late Pleistocene terraces correspond to surfaces mapped by *Peltier* [1949] and *Engel et al.* [1996]. The location of this cross section is shown in Figure 2.

cross-section view for a location south of Muncy (RK 41) where the terraces are particularly evident (Figure 7). The Quaternary terrace elevation designations are from *Engel et al.* [1996], and the cross section location is near the Muncy location as described in *Engel et al.* [1996]. Comparing *Engel et al.* [1996] and *Peltier* [1949], the Qt5a terrace deposits are similar in age to the Valley Heads terrace in *Peltier* [1949]. The Qt4 age is similar to that of the Binghamton terrace, Qt4a is similar to the Olean terrace, and Qt3 is similar in age to the Late Illinoian terrace.

8.2. Channel Shear Stress Variability

The channel shear stresses vary greatly between Muncy and Northumberland. This variation is presented in Figure 8a as a profile of shear stress values taken along the modern thalweg of the West Branch. For comparison, the graph also shows the estimated critical shear stress of sediment with a 64 mm diameter and 128 mm diameter as 20 N/m^2 and 42 N/m^2, respectively. These sediment sizes represent the median and d_{84} sediment sizes from the pebble count sample with the largest grain sizes collected near Milton, PA. The dimensionless critical shear stress parameter was assumed to be 0.05 [*Gordon et al.*, 2004]. Similar to the water-surface elevations (Figure 6), the paleoflood peak discharges result in a similar pattern of variability; yet the modern 100 year peak discharge does not follow this same pattern. In general, the paleofloods resulted in higher bed shear stresses with increased simulated discharges as would be expected. However, there are several reaches (near RK 45 and RK 15 to 10) where the modern 100 year peak discharge resulted in higher shear stresses than the estimated paleoflood discharges. In both of these cases, the main contributing factor is related to backwater effects upstream of topographic constrictions. These topographic constrictions cause a significant contraction of flow that is large enough to create an upstream rise in water-surface elevation for the higher paleoflood discharges, but the lower modern 100 year flood discharge volume is not large enough for the topographic constriction to cause significant flow contraction and therefore, upstream backwater effects. Figure 8b shows detail of the shear stress profile near Lewisburg. From RK 15.5 to 10.5, the modern 100 year peak discharge results in the highest bed shear stresses. For the paleoflood discharges, the lowest peak discharge estimate results in the highest shear stresses from RK 19 to 10.5.

Where the shear stress is high for the paleoflood discharges, the modern 100 year flood discharge does not always show an increase in shear stress. For example, see RK 35 in Figure 8a. The topography near RK 35

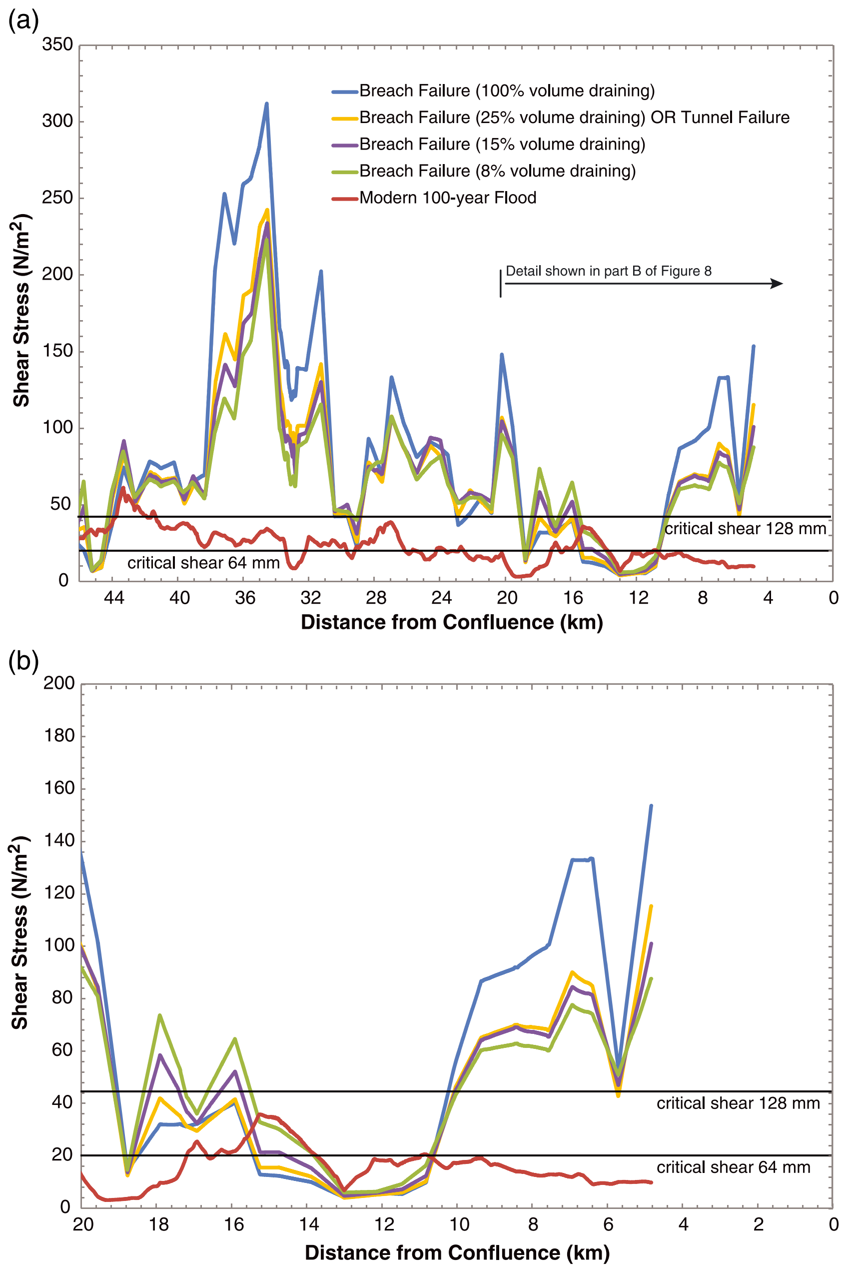

Figure 8. (a) Channel shear stress profile for the entire study reach and (b) detail of shear stress variation near Lewisburg, PA.

creates a fairly long constriction where paleoflood shear stresses are greatly increased. Similar to the backwater effect, the topographic constrictions themselves are not tight enough to contract the flow of the much lower modern 100 year discharge volume.

8.3. Areal Flood Inundation

The resulting flood inundation areas for the modern 100 year peak discharge and the paleoflood estimates are compared with surficial geology maps [*Faill*, 1979; *Marchand and Crowl*, 1991; *Inners*, 1997]. In general, the modern 100 year peak discharge inundates areas underlain by Holocene alluvium ("al") and modern flood deposits. The paleoflood estimates extend the inundation area to include areas underlain by identified middle and late Pleistocene sediments. Figures 9 and 10 compare several inundation areas near the confluence with White Deer Creek and near Lewisburg with the surficial geology map developed by

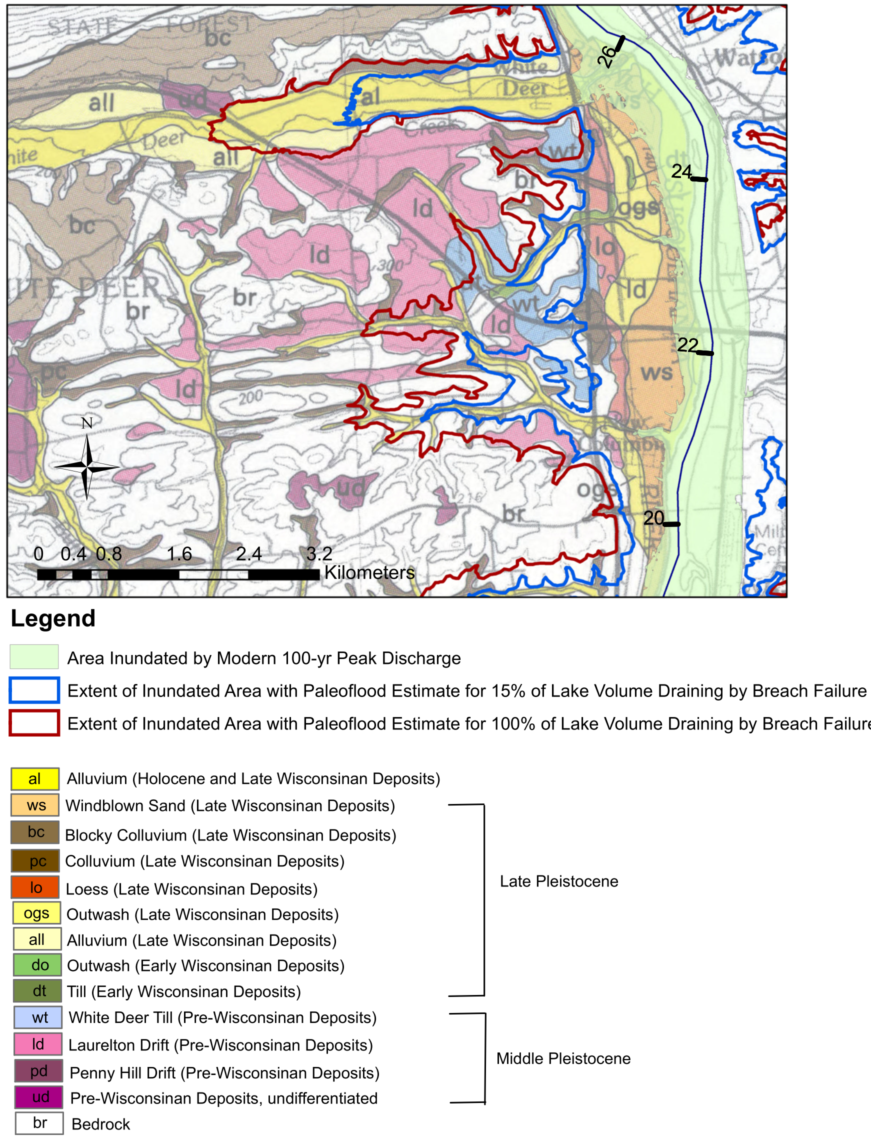

Figure 9. Map of surficial geology and flood inundation estimates from HEC-geoRAS postprocessing near the confluence with White Deer Creek. The underlying map and the description of map units are from *Marchand and Crowl* [1991]. Note that surficial mapping data are not available on the east side of the West Branch; therefore, only the west side of the river is shown for this comparison.

Marchand and Crowl [1991]. The *Marchand and Crowl* [1991] map provides more specific detail on the age of the identified surficial deposits than the surficial geology maps developed by *Faill* [1979] and *Inners* [1997]; however, the *Marchand and Crowl* [1991] map only covers the western side of the West Branch from Watsontown, PA, to the confluence at Northumberland, PA. Near the confluence of the West Branch with White Deer Creek (Figure 9), the paleoflood discharge estimates assuming 15% and 100% of the lake volume drained by breach failure both inundate surficial deposits identified as late Pleistocene aged. More specifically "ogs" or outwash sediments are inundated by both paleoflood estimates near the White Deer Creek confluence. Areas near the West Branch channel with middle Pleistocene deposits (mainly, "wt": White Deer till and some "ld": Laurelton drift) are inundated by the highest paleoflood estimate. Given the description of the ld deposits by *Marchand and Crowl* [1991], the Laurelton drift is mainly till but does include local glaciofluvial and lacustrine deposits. Areas farther from the main channel with ld deposits are not inundated by the paleoflood estimates in the location near the White Deer Creek confluence. Near Lewisburg (Figure 10), a large area of ogs deposit is inundated by both paleoflood estimates. Late

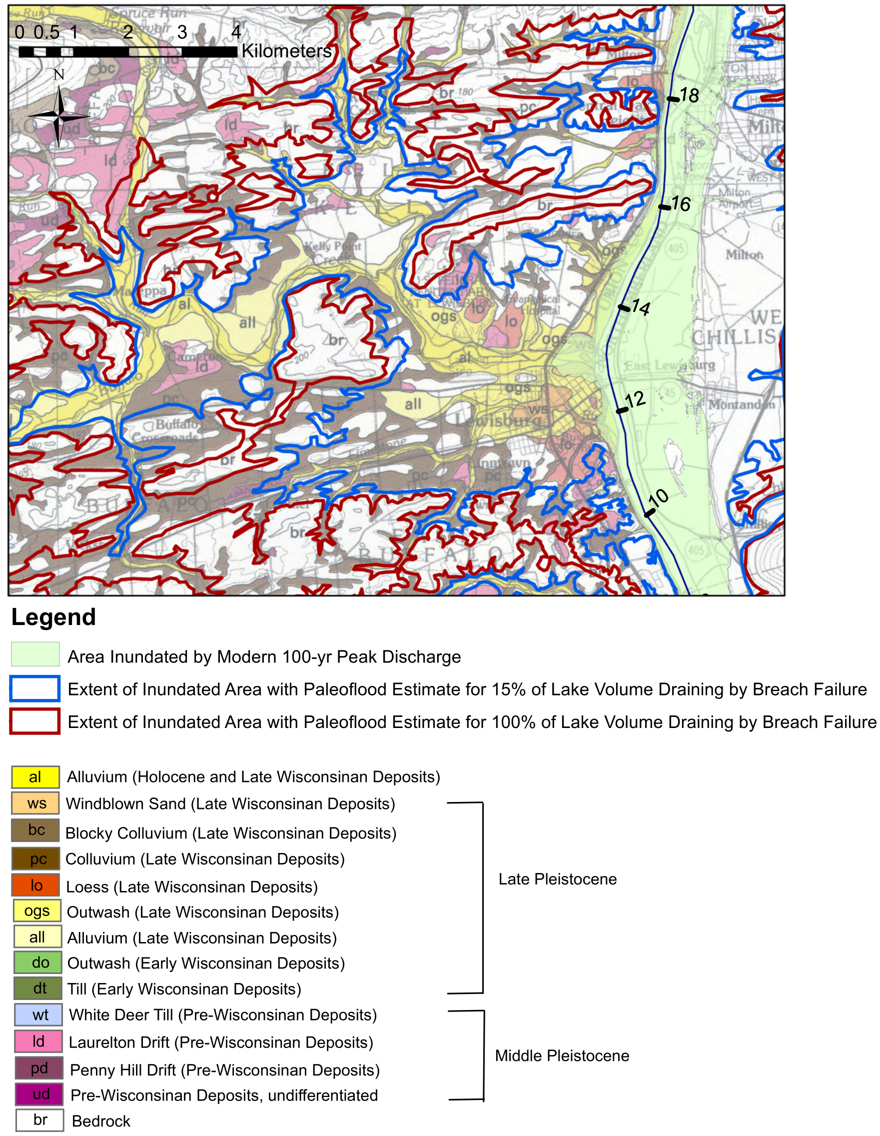

Figure 10. Map of surficial geology and flood inundation estimates from HEC-geoRAS postprocessing near Lewisburg. The underlying map and the description of map units are from *Marchand and Crowl* [1991]. Note that surficial mapping data are not available on the east side of the West Branch; therefore, only the west side of the river is shown for this comparison.

Pleistocene alluvium deposits ("all") also are inundated by both paleoflood estimates. In this location, many of the areas with Laurelton drift (ld) are inundated by the both paleoflood peak discharge estimates.

9. Conclusions

The hydraulic modeling results support hypotheses of the occurrence of glacial dam-break floods on the West Branch of the Susquehanna River during the Pleistocene period. The exact location of the ice dam, frequency of its failure, and the amount of lake volume drainage during failure remain in question. However, the paleoflood discharge estimates are reasonable and compare favorably to the geological evidence of glacial outburst floods, such as the elevations of the Pleistocene terraces and areal extents of outwash sediments mapped by previous researchers. The computed water-surface profiles (Figures 6 and 7) and channel shear stresses (Figures 8) could explain the erosional and depositional features formed during the Pleistocene [*Peltier*, 1949; *Engel et al.*, 1996].

The hydraulic model shows that water depths and areal extent of flooding associated with the Pleistocene outburst floods were great enough that valley constrictions caused significant backwater effects immediately upstream. The water-surface profiles for the paleoflood estimates (Figure 6) show a flat water surface between RK 18 and 10, indicating the longitudinal extent of backwater due to the constriction at Montour Ridge. Ice jams at these valley constrictions would have only increased the backwater flooding. The model also shows that modern rainfall-runoff floods, such as the 100 year event, are much smaller than the Pleistocene ice-dam outburst floods, and they are not affected by valley constrictions nor do they experience backwater effects.

Additional evidence of these topographic controls on the glaciofluvial processes versus modern fluvial processes is demonstrated by the bed profile that was created from the collection of bathymetry data in the West Branch (Figure 3). For the greater smoothing of the raw bed elevation data, the pool-riffle sequence from RK 18 to RK 10 is muted. If the greater smoothing reveals larger-scale bed features due to formation by a paleoflood regime, this lack of larger pools and riffles could correspond to the large backwater effect that is evident in this section based on paleoflood simulations and surficial geology maps [*Marchand and Crowl*, 1991]. The smaller pools and riffles that are evident with the lower amount of smoothing of the raw bed elevation data (Figure 3) could be due to the smaller modern flow regime that does not show backwater effects in this reach.

The flood inundation maps superimposed on the surficial geology map of *Marchand and Crowl* [1991] provide further support for the simulated backwater effects upstream of a valley constriction near Lewisburg, PA, where the paleofloods appear to inundate the areas where the Laurelton drift (ld) and other glaciofluvial sediment (ogs) deposits have been identified. If backwater effects are large enough, a lake-like environment could have been created in this region. For the section of river where White Deer Creek enters, the paleoflood inundation maps also show some agreement with the surficial geology map [*Marchand and Crowl*, 1991] where outwash sediments (ogs) are inundated. However, there are large deposits identified as Laurelton drift (ld) that are not inundated even by the maximum paleoflood estimate with 100% of the lake volume draining by breach failure. This discrepancy could be due to a number of factors, mainly, that only the main West Branch is modeled by the one-dimensional HEC-RAS and the flow additions at tributary confluences are not considered. The Laurelton drift deposits near the White Deer Creek confluence could be the result of flow hydraulics at this confluence that cannot be simulated by a one-dimensional model on only the West Branch and could suggest that tributaries contributed some flow to the West Branch in addition to the flow from a dam-break scenario from glacial Lake Lesley.

The hydraulic simulation of estimated paleoflood discharges on the West Branch of the Susquehanna River enables additional analysis of potential glaciofluvial processes and their effect on the current river bed form. When combined with previously compiled geological evidence of glacial Lake Lesley and a higher paleoflood regime [*Peltier*, 1949; *Nelson*, 1965; *Faill*, 1979; *Marchand and Crowl*, 1991; *Engel et al.*, 1996; *Inners*, 1997; *Ramage et al.*, 1998; *Hayes*, 2001; *Kochel et al.*, 2009], a more complete view of the potential geomorphic significance of paleofloods is possible.

Acknowledgments
The lidar data are available on the Pennsylvania Spatial Data Access (PASDA) site: www.pasda.psu.edu. The collected West Branch bathymetry data are available from the authors upon request. Equipment and student support for this study were funded by the Bucknell Program for Undergraduate Research, the Bucknell Center for Sustainability and the Environment, and the Degenstein Foundation. The authors would like to thank R. Craig Kochel for the helpful discussion; Sean P. Reese, Kayla Yee, and Molly Gutelius for their assistance with field data collection; and Janine Glathar for assistance with GIS data processing.

References

Ackerman, C. T. (2009), HEC-geoRAS, GIS tools for the support of HEC-RAS using ArcGIS, User's Manual, U.S. Army Corps of Engineers CPD-83.

Alho, P., and J. Aaltonen (2008), Comparing a 1D hydraulic model with a 2D hydraulic model for the simulation of extreme glacial outburst floods, *Hydrol. Processes*, *22*, 1537–1547, doi:10.1002/hyp.6692.

Alho, P., A. J. Russell, J. L. Carrivick, and J. Käyhkö (2005), Reconstruction of the largest Holocene jökuhlaup within Jökulsá á Fjöllum, NE Iceland, *Quat. Sci. Rev.*, *24*, 2319–2334, doi:10.1016/j.quascirev.2004.11.021.

Alho, P., V. R. Baker, and L. N. Smith (2010), Paleohydraulic reconstruction of the largest glacial Lake Missoula draining(s), *Quat. Sci. Rev.*, *29*, 3067–3078, doi:10.1016/j.quascirev.2010.07.015.

Baker, V. R. (2009), Overview of megaflooding: Earth and Mars, in *Megaflooding on Earth and Mars*, edited by D. M. Burr et al., Cambridge Univ. Press, Cambridge, U. K.

Bohorquez, P., and S. E. Darby (2008), The use of one- and two-dimensional hydraulic modeling to reconstruct a glacial outburst flood in a steep Alpine valley, *J. Hydrol.*, *361*, 240–261, doi:10.1016/j.jhydrol.2008.07.043.

Brunner, G. W. (2010), HEC-RAS River Analysis System User's Manual, Version 4.1, U.S. Army Corps of Engineers CPD-68.

Carling, P. A., I. Villanueva, J. Herget, N. Wright, P. Borodavko, and H. Morvan (2010), Unsteady 1D and 2D hydraulic models with ice dam break for Quaternary megaflood, Altai Mountains, southern Siberia, *Global Planet. Change*, *70*, 24–34, doi:10.1016/j.gloplacha.2009.11.005.

Carravick, J. L., and F. S. Tweed (2013), Proglaical lakes: Character, behavior and geological importance, *Quat. Sci. Rev.*, *78*, 34–52, doi:10.1016/j.quascirev.2013.07.028.

Cenderelli, D. A., and E. E. Wohl (2001), Peak discharge estimates of glacial-lake outburst floods and “normal” climatic floods in the Mount Everest region, Nepal, *Geomorphology*, *40*, 57–90.

Cenderelli, D. A., and E. E. Wohl (2003), Flow hydraulics and geomorphic effects of glacial-lake outburst floods in the Mount Everest region, Nepal, *Earth Surf. Processes Landforms*, *28*, 385–407, doi:10.1002/esp.448.

Costa, J. E., and R. L. Schuster (1988), The formation and failure of natural dams, *Geol. Soc. Am. Bull.*, *100*, 1054–1068.

Denlinger, R. P., and D. R. H. O’Connell (2010), Simulations of cataclysmic outburst floods from Pleistocene Glacial Lake Missoula, *Geol. Soc. Am. Bull.*, *122*(5/6), 678–689, doi:10.1130/B26454.1.

Driedger, C. L., and A. G. Fountain (1989), Glacier outburst floods at Mount Ranier, Washington State, U.S.A., *Ann. Glaciol.*, *13*, 51–55.

Engel, S. A., T. W. Gardner, and E. J. Ciolkosz (1996), Quaternary soil chronosequences on terraces of the Susquehanna River, Pennsylvania, *Geomorphology*, *17*, 273–294.

Faill, R. T. (1979), *Geology and Mineral Resources of the Montoursville South and Muncy Quads, Lycoming, Northumberland, and Montour Counties, PA, Atlas 144ab*, Pennsylvania Geol. Surv., Harrisburg, Pa.

Fountain, A. G., and J. S. Walder (1998), Water flow through temperate glaciers, *Rev. Geophys.*, *36*, 299–328, doi:10.1029/97RG03579.

Gordon, N. D., T. A. McMahon, B. Finlayson, C. J. Gippel, and R. J. Nathan (2004), *Stream Hydrology: An Introduction for Ecologists*, John Wiley, U. K.

Hayes, B. R. (2001), Geophysical mapping of hydrostratigraphy of valley fill sediments underlying a palustrine wetlands adjacent to the Susquehanna River, Northumberland County, Pennsylvania, Abstracts with Programs, 2001 Annual Meeting of Geological Society of America, Boston, Mass., 5–8 Nov.

Hewitt, K., and J. Liu (2010), Ice-dammed lakes and outburst floods, Karakoram Himalaya: Historical perspectives on emerging threats, *Phys. Geogr.*, *31*(6), 528–551.

Hunt, J., G. Brunner, and B. Larock (1999), Flow transitions in bridge backwater analysis, *J. Hydraul. Eng.*, *125*(9), 981–983.

Inners, J. D. (1997), *Geology and Mineral Resources of the Allenwood and Milton Quads, Union and Northumberland Counties, PA, Atlas 144cd*, Pennsylvania Geol. Surv., Harrisburg, Pa.

Kasse, C. (2014), Fluvial response to rapid high-amplitude lake-level changes during the Late Weichselian and early Holocene, Ain River valley, Jura, France, *Boreas*, *43*, 403–421, doi:10.1111/bor.12058.

Kidson, R. L., K. S. Richards, and P. A. Carling (2006), Hydraulic model calibration for extreme floods in bedrock-confined channels: Case study from northern Thailand, *Hydrol. Processes*, *20*, 329–344.

Klimeš, J., M. Benešová, V. Vilímek, P. Bouška, and A. C. Rapre (2014), The reconstruction of a glacial lake outburst flood using HEC-RAS and its significance for future hazard assessments: An example from Lake 513 in the Cordillera Blanca, Peru, *Nat. Hazards*, *71*, 1617–1638, doi:10.1007/s11069-013-0968-4.

Kochel, R. C., R. P. Nickelsen, and L. S. Eaton (2009), Catastrophic middle Pleistocene jökulhlaups in the upper Susquehanna River: Distinctive landforms from breakout floods in the central Appalachians, *Geomorphology*, *110*, 80–95, doi:10.1016/j.geomorph.2009.03.025.

Lee, J. (2013), A survey of transverse drainages in the Susquehanna River basin, Pennsylvania, *Geomorphology*, *186*, 50–67.

Marchand, D. E., and G. H. Crowl (1991), Surficial geology map of parts of Union and Snyder counties, Pennsylvania, Map I-2051, Scale 1:100,000, U.S. Geol. Surv. Misc. Invest. Ser., Pa.

Mayo, L. (1989), Advance of Hubbard Glacier and 1986 outburst of Russell Fjord, Alaska, U.S.A., *Ann. Glaciol.*, *13*, 189–194.

Meinsen, J., J. Winsemann, A. Weitkamp, N. Landmeyer, A. Lenz, and M. Dölling (2011), Middle Pleistocene (Saalian) lake outburst floods in the Münsterland Embayment (NW Germany): Impacts and magnitudes, *Quat. Sci. Rev.*, *30*, 2597–2625, doi:10.1016/j.quascirev.2011.05.014.

Motyka, R. J., and M. Truffer (2007), Hubbard Glacier, Alaska: 2002 closure and outburst of Russell Fjord and postflood conditions at Gilbert Point, *J. Geophys. Res.*, *112*, F02004, doi:10.1029/2006JF000475.

Nelson, J. G. (1965), Some effects of glaciation on the Susquehanna River Valley, *Ann. Assoc. Am. Geogr.*, *55*(3), 404–448.

Newlin, J. T., B. R. Hayes, and K. Yee (2013), Morphologic investigation of the West Branch of the Susquehanna River in north-central Pennsylvania, World Environmental and Water Resources Congress 2013, Cincinnati, pp. 2261–2270, Ohio, doi:10.1061/9780784412947.222, 19–23 May.

Peltier, L. (1949), Pleistocene terraces of the Susquehanna River, Pennsylvania, Pennsylvania Geol. Surv. Bull. G23, p. 177.

Ramage, M. J., T. W. Gardner, and D. I. Sasowsky (1998), Early Pleistocene glacial Lake Lesley, West Branch Susquehanna River valley, central Pennsylvania, *Geomorphology*, *22*, 19–37.

Roberts, M. J. (2005), Jökulhlaups: A reassessment of floodwater through glaciers, *Rev. Geophys.*, *43*, RG1002, doi:10.1029/2003RG000147.

Rudoy, A. N. (2002), Glacier-dammed lakes and geological work of glacial superfloods in the Late Pleistocene, Southern Siberia, Altai Mountains, *Quat. Int.*, *87*, 119–140.

Sevon, W. D. (1993), River on a rampage, *Pennsylvania Geology*, *24*(2), 2–7.

Sevon, W. D., G. M. Fleegor, and V. C. Shepps, (1999), Pennsylvania and the ice age, Education Series 6, Pennsylvania Geol. Surv., Harrisburg, Pa.

Sheffer, N. A., M. Rico, E. Yehouda, G. Benito, and T. Grodek (2008), The paleoflood record of the Gardon River, France: A comparison with the extreme 2002 flood event, *Geomorphology*, *98*, 71–83, doi:10.1016/j.geomorph.2007.02.034.

Tweed, F. S., and A. J. Russell (1999), Controls on the formation and sudden drainage of glacier-impounded lakes: Implications for jökulhlaup characteristics, *Prog. Phys. Geogr.*, *23*, 79–110.

Walder, J. S., and J. E. Costa (1996), Outburst floods from glacier-dammed lakes: The effect of mode of lake drainage on flood magnitude, *Earth Surf. Processes Landforms*, *21*, 701–723.